

Cross-sectional uncertainties influences on sensitivity studies of DUNE and T2HK experiments

Ritu Devi^{1*}, Jaydip Singh^{2†}, Baba Potukuchi^{1‡}

Department Of Physics, University of Jammu, Jammu, India¹ and

Department Of Physics, University of Lucknow, Lucknow, India.²

The ultimate objectives of ongoing and upcoming neutrino experiments are the precise measurement of neutrino mixing parameters and the confirmation of mass hierarchy. The systematic inaccuracy in the cross-section models introduces inaccuracy in the neutrino mixing parameters estimation. It is important to secure a large decrease of uncertainties, particularly those relating to cross-section, neutrino-nucleus interactions, and neutrino-energy reconstruction, in order to achieve these ambitious goals. In this research article, we use three alternative neutrino event generators, GENIE, NuWro, and GiBUU, to analyze sensitivity studies of T2HK, DUNE, and combined sensitivity of DUNE, and T2HK for mass hierarchy, CP violation, and octant degeneracy caused by cross-section uncertainties. The cross-section models of these generators are separate and independent.

1. Introduction

Neutrino oscillation physics is a well-established field of study that has faced numerous obstacles in recent decades. However, with the help of a number of remarkable experiments, significant progress has been made in the field of neutrino oscillation physics. Neutrino oscillation is the change in neutrino flavor as they travel, i.e., a neutrino that starts off with one flavor may finish up with a different flavor after a certain distance. Mixing angles θ_{ij} , where $i < j = 1, 2, 3$ ($\theta_{23}, \theta_{12}, \theta_{13}$), Dirac phase δ_{CP} , and the size of mass squared differences, Δm_{21}^2 for solar mass splitting and Δm_{31}^2 for atmospheric mass splitting, are neutrino oscillation parameters that influence neutrino oscillation physics. The near-perfect measurement of the mixing angles θ_{23}, θ_{12} and non-zero value of θ_{13} [1–3] as well as mass squared discrepancies has made substantial progress in the exact computation of neutrino oscillation parameters. There are, however, a number of issues that are to be resolved and these are-(i) the sign of Δm_{31}^2 i.e. neutrino mass hierarchy or ordering of neutrino mass. For the neutrino mass eigenstates m_i ($i=1, 2, 3$), there are two possible configurations. The first is Normal Ordering (NO), also known as the Normal Hierarchy (NH), in which $m_1 < m_2 < m_3$, and the second is Inverted Ordering (IO), also known as the Inverted Hierarchy (IH), in which the neutrino mass order is $m_2 \approx m_1 > m_3$ (ii) calculation of the octant of θ_{23} that refers to whether θ_{23} lies in $0 < \theta_{23} < \pi/4$ i.e. lower octant (LO) or in $\pi/4 < \theta_{23} < \pi/2$ i.e. higher octant (HO). This refers to the octant degeneracy problem of θ_{23} (iii) estimation of the value of the CP-violating phase δ_{CP} , which can lie anywhere between $-\pi < \delta_{CP} < \pi$. As we know that CP conservation is represented by the values 0 and $\pm 180^\circ$, while maximal CP violation is represented by the

* E-mail: rituhans4028@gmail.com

† E-mail: jaydip.singh@gmail.com

‡ E-mail: baba.potukuchi@gmail.com

value $\pm 90^\circ$. This discovery may offer insight into the origins of leptogenesis [4] and may be used to answer several important puzzles, such as the universe's baryon asymmetry [5].

A variety of factors influence our understanding of neutrino oscillation physics, the most crucial of which is the precise reconstruction of neutrino energy. Because the probability of neutrino oscillation is directly proportional to their energy, any error in neutrino energy measurement will affect measurements of neutrino oscillation parameters, causing inaccuracies in cross-section measurement and event identification. Several notable long-baseline neutrino oscillation investigations use accelerator-produced neutrino beams. Because these neutrino beams are not monoenergetic, complete information on final state particles is needed to reconstruct neutrino energy. Identifying final state particles in the influence of nuclear effects is difficult because the particles formed at the initial neutrino-nucleon interaction vertex and the particles collected by the detector can be different or not identical. Heavy nuclear targets are used in current and anticipated future neutrino oscillation experiments to capture huge event statistics, which is a priori necessity of neutrino oscillation studies, but they also amplify nuclear effects [6]. The statistical error is minimized as a result of the vast event statistics obtained, and attention is directed to finding a way to handle systematic errors. One of the most common sources of systematic errors is uncertainty in the determination of neutrino-nucleus cross-sections due to the existence of nuclear effects. In order to decrease systematic inaccuracies, it is critical to investigate the precise neutrino-nucleon interaction cross-sections. The link between uncertainties in neutrino-nucleon cross-sections and their impact on the calculation of neutrino oscillation parameters has been studied extensively [7–9]. As indicated in [10–15], existing knowledge of nuclear impacts is insufficient to control systematic errors.

In this paper, we have chosen three alternative simulation tools, GENIE (Generates Events for Neutrino Interaction Experiments) [16], NuWro [17], and GiBUU (Giessen Boltzmann-Uehling-Uhlenbeck) [18], in order to represent nuclear effects and investigate the sensitivity of the T2HK (Tokai to Hyper-Kamiokande) and DUNE (Deep Underground Neutrino Experiment) in resolving mass hierarchy, octant degeneracy, and CP violation. Nuclear effects are included in all three neutrino event generators' simulation codes, however, there are differences in the nuclear models used and the calculation of various neutrino-nucleus interaction processes. The nucleus is made up of nucleons, and it is not easy to figure out how all of them engage in neutrino-nucleus interactions. Different approximations are used to define nuclear effects by different neutrino event generators that incorporate nuclear effects in their analysis procedure. Because the outcome of an experiment must be model-independent, this inspired us to do our analysis.

The following sections comprise the paper: In Section 2, we discuss the NuWro, GENIE, and GiBUU neutrino event generators that were employed in this study, as well as a full comparison of their physics. In Section 3, we go over the simulation and experimental details, then in Section 4, we go over the octant sensitivity, mass hierarchy, and CP sensitivity results. Finally, Section 5, gives our summary and conclusions.

2. Simulation tools: GENIE, NuWro and GiBUU

GENIE 3.00.06 [16], NuWro version 19.01 [17], and GiBUU v-2021 [18] are three neutrino event generators employed in this study to determine the interaction cross-section ($\nu - Ar$) and ($\nu - H_2O$). We looked at the interaction mechanisms of quasi-elastic (QE), resonance (RES) from resonant decay, two particle-two hole (2p2h/MEC), and deep inelastic scattering (DIS). The total cross-section computed from the three generators is then converted to the

GLOBES (General Long Baseline Experiment Simulator) package’s input format. Figure 1 shows the neutrino cross-section as a function of neutrino energy for both Ar and H_2O targets. We see a large difference in the value of cross-sections for $(\nu - Ar)$ calculated using GiBUU but a small difference when calculated using GENIE and NuWro. GiBUU shows higher cross-section for energy range 0.05-1 GeV and lower cross-section for energy range 1-10 GeV. In the case of $\nu - H_2O$, all generators show different cross-section. NuWro shows lower cross section as comparison to GENIE and GiBUU in the energy range 0.05-1 GeV. For the energy range 1-10 GeV, Nuwro shows higher cross-section but GENIE and GiBUU show lower cross-section.

In this section, we will go over the qualitative theoretical differences in nuclear models, as well as how neutrino-nucleus interaction processes are accounted for in all generators and some popular approaches to neutrino-nucleus interaction analysis. In terms of nuclear models explaining neutrino-nucleus interactions, the selected event generators differ.

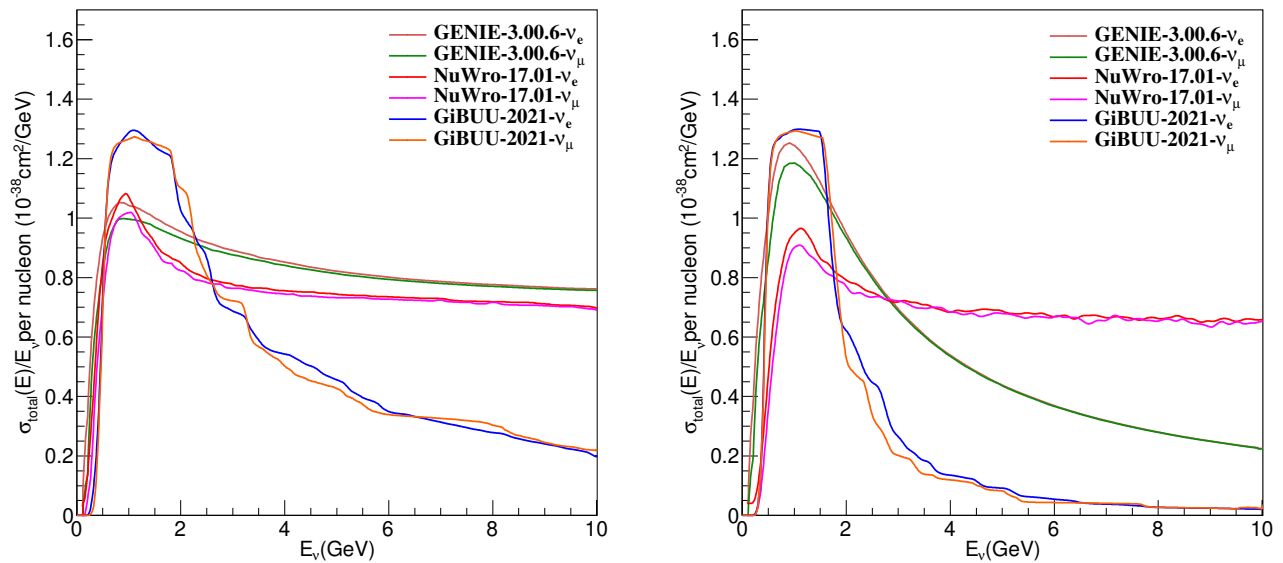


Figure 1: Total ν -Ar (left panel) and ν - H_2O (right panel) interaction cross-section per nucleon as a function of true neutrino energy for GENIE, NuWro, and GiBUU.

- GENIE:** GENIE [16] is a neutrino event generator based on ROOT [19] that was written entirely in C++ utilizing object-oriented approaches. MINERvA [20], MINOS [21], MicroBooNE [22], NovA [23], and T2K are only a few of the neutrino baseline experiments that employ it around the world. For all processes, the Relativistic Fermi Gas (RFG) nuclear model is utilized. GENIE employs Bodek and Ritchie’s version, which has been tweaked to include short-range nucleon-nucleon correlations [24]. In GENIE, QE scattering is simulated by the Llewellyn-Smith model [25] with BBBA05 [26]. The Rein-Sehgal model [27] includes the creation of baryon resonances in neutral current (NC) and charged current (CC) channels. The Feynman-Kislinger-Ravndal [28] model of baryon resonances is used in this model. GENIE has 16 resonance modes out of 18 resonance. At neutrino energies smaller than 1 GeV, processes involving two particle two hole (MEC/2p2h) excitations give an additional contribution to the overall neutrino cross-section. The nucleon-nucleon correlations in the initial state interactions (ISI), neutrino coupling to the 2p2h, and FSI all play a role in this process. Simulation of DIS

processes in GENIE is according to Bodek and Yang model [29]. The axial mass in GENIE is variable, ranging from 0.99 to 1.2 GeV/c^2 .

- **NuWro:** NuWro [17] was developed at the University of Wroclaw and has now evolved into a valuable sandbox for other generators, presenting novel theoretical models that are tested before being incorporated by NEUT and GENIE. For the QE process, NuWro uses fundamental Llewellyn Smith formulas [25], with a wide range of vector form factor possibilities (dipole, BBA03 [30], BBBA05 [26], Alberico et al [31]). Typically, global and local relativistic FG models or the spectral function (SF) method are utilized. With nucleon- Δ form factors for RES events given from Ref. [32], only the Δ resonance is explicitly provided, with $C_A^5(0)=1.19$ as the free parameter and for the rest of the resonance modes, we have an average based on the Adler-Rarita-Schwinger model [32] for RES events. For simulation of the DIS channel ($W > 1.6GeV$), the Bodek-Yang prescription [34] is used to analyze the total cross-sections. For specified quark configurations, the Pythia6 hadronization routine is used to allow their employment in the low W area down to 1.2 GeV.
- **GiBUU:** With a single, consistent physics model, GiBUU [18] intends to represent a large number of different nuclear processes (electron, proton, photon, pion, neutrino, A)-A over a wide range of energies. It employs FORTRAN procedures. Ref. [18] contains the most detailed description of the model. RFG model in GiBUU is updated by including a density-dependent mean-field potential term that assumes all nucleons are bound. Ref.[12, 35] provides more information on the QE cross-section process in GiBUU. $M_A = 1GeV/c^2$ is the axial mass employed by GiBUU. The impulse approximation is used to model true CCQE (charged current quasi-elastic) neutrino interactions with single nucleons. For the axial component, a typical dipole form is utilized, while the BBBA07 [36] parameterization is used for the vector form factors. Based on the kinematics of the final state nucleons, the computation also employs a density-dependent Pauli-blocking of interactions. There are 13 different types of resonance modes in GiBUU. MAID analysis of electron scattering data [37, 38] yields vector form factors for each of GiBUU's 13 resonance modes. Simulation of DIS process in GiBUU is done by PYTHIA6 [39].

3. Experimental details for the simulation studies

We simulated the tests alone and combined them to better understand the sensitivities and complementarity of DUNE and T2HK. We are using the GLOBES libraries [40, 41], which require cross-section, neutrino, and anti-neutrino beam fluxes, and detector parameterization parameters as input. The cross-section input format is $\hat{\sigma}(E) = \sigma(E)/E[10^{-38}cm^2/GeV]$, and more information can be found in [42]. The experimental specifications for the DUNE and T2HK setups that we employed in our analysis are listed below.

- **T2HK:** The T2HK experiment [43] is a proposed next-generation long-baseline experiment that will use a neutrino beam generated at J-PARC in Tokai and directed 2.5 degrees off-axis to Hyper-Kamiokande (Hyper-K). The target power is supposed to be 4 MW, with a running period of 5 years for an antineutrino beam and 5 years for a neutrino beam. The planned HyperKamiokande detector, with a fiducial mass of 500 kton and a baseline length of 295 km, is used as a detector. The narrow-band beam is largely made up of ν_μ (or $\bar{\nu}_\mu$), with

a peak energy of 0.6 GeV, which corresponds to the first oscillation maximum at 295 km. At this energy range QE is the most prevalent process which itself have systematics from 2p2h/MEC channels [46]. For simulation, our input files for T2HK is based on the GLoBES package, which has been extensively modified to meet the most recent experimental design. In both signal and background normalization, we account for 5% uncertainty. [45]. The energy resolution for both ν_e and ν_μ is $8.5\%/\sqrt{E}$ GeV.

- **DUNE:** DUNE at LBNF (Long-Baseline Neutrino Facility) will be made up of near detector (ND) and far detector (FD) with the same Argon (Ar) material, but the proportions and technology will change. The ND system will be positioned 574 meters downstream and 60 meters underground [47] from the neutrino beam source site at Fermilab. We assumed a FD with a fiducial volume of 40 kton liquid argon ($A = 40$) located at a distance of $L = 1300$ km from the wide-band neutrino beam source and an operating time of 5 years in both neutrino and antineutrino mode for the simulation of DUNE experiment. The DUNE-LBNF flux has an average energy of 2.5 GeV and the RES process is the most prevalent process at this energy. The neutrino flux employed in this study corresponds to the 80 GeV Reference beam configuration [48], with a beam power of 1.07 MW. An energy smearing technique, which we decided to be a Gaussian function of energy resolution, is used to compute binned event rates [42]. The energy resolution for ν_e is $15\%/\sqrt{E}$ (GeV), while for ν_μ it is $20\%/\sqrt{E}$ (GeV) [49]. We account for 5% uncertainty in signal and 10% in background normalization. Table I shows the true values of the oscillation parameters [50] considered in this study.

Table I: Oscillation parameters included in our analysis.

Parameter	Best Fit Value	3σ Range
θ_{12}	0.590	-
θ_{13}	0.151	-
$\theta_{23}(\text{NH})$	0.867	0.703-0.914
$\theta_{23}(\text{IH})$	0.870	0.710-0.917
δ_{CP}	0	$-\pi - +\pi$
Δm_{21}^2	$7.39\text{e-}5\text{eV}^2$	-
$\Delta m_{31}^2(\text{NH})$	$2.525\text{e-}3\text{ eV}^2$	$+2.427 \rightarrow +2.625$
$\Delta m_{31}^2(\text{IH})$	$-2.512\text{e-}3\text{ eV}^2$	$-2.611 \rightarrow -2.412$

4. Sensitivity studies

In this section, we attempted to investigate the impact of cross-sectional uncertainties (deficiencies in the theoretical aspects of nuclear physics models as implied by the generators) on the three key goals of DUNE and T2HK, namely (i) CP phase violation, (ii) mass ordering, and (iii) octant degeneracy. Several attempts have been made to perform the sensitivity analysis, for example, complete sensitivity analysis for other experiments like T2K [51], T2HK [52], NOvA [23] along with DUNE in [53–55].

4.1. CP violation sensitivity with DUNE and T2HK

To detect CP violation, the CP phase value must be different from CP preserving values, such as 0 or $\pm\pi$. Because the true value of δ_{CP} is unknown, the analysis is carried out by scanning all possible true values of δ_{CP} over the complete range $-\pi < \delta_{CP} < +\pi$ and comparing them to the δ_{CP} conserving values. δ_{CP} , θ_{23} and $|\Delta m_{31}^2|$ are our test parameters. We minimized over the test parameters in the 3σ range when doing our analysis, as shown in Table I. We do the following computations to get the CP violation sensitivity:

$$\Delta\chi_0^2 = \chi^2(\delta_{CP} = 0) - \chi_{true}^2 \quad (1)$$

$$\Delta\chi_\pi^2 = \chi^2(\delta_{CP} = \pi) - \chi_{true}^2 \quad (2)$$

$$\Delta\chi^2 = \min(\Delta\chi_0^2, \Delta\chi_\pi^2) \quad (3)$$

Using $\sigma = \sqrt{\Delta\chi^2}$, a qualitative handle on the measurement of CP violation is acquired, as shown in the Fig. 2.

When NH is considered actual hierarchy, CP sensitivity is shown in the left panel of Fig.2. In the negative half range, $(-1 < \delta_{CP}/\pi < 0)$ we see around 1σ difference between GENIE and NuWro but there is a small difference between GiBUU and NuWro for the T2HK experiment and in the case of DUNE experiment, GENIE and NuWro show similar results but GiBUU shows some variations at $\delta_{CP} \sim -0.5/\pi$. When we combine DUNE+T2HK, we see a small difference in GENIE but GiBUU and NuWro show similar results at $\delta_{CP} \sim -0.5/\pi$. In the case of the positive

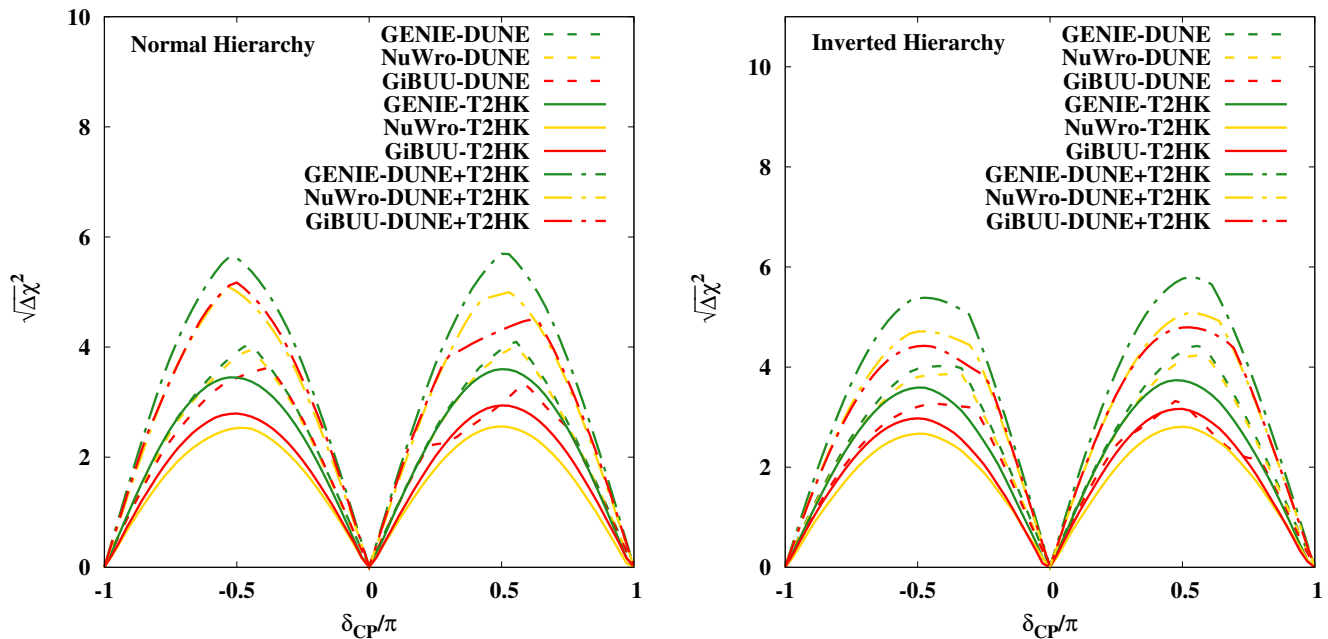


Figure 2: CP sensitivity measurement as a function of the true value of δ_{CP} for NH (left panel) and IH (right panel) by GENIE (green lines), NuWro (yellow lines), and GiBUU (red lines) for T2HK, DUNE, and T2HK+DUNE experiments.

half ($0 < \delta_{CP}/\pi < 1$), we notice a 1σ difference between GENIE and NUWro for the T2HK experiment but for the DUNE experiment, we notice GENIE and NuWro show identical results but GiBUU shows around 1σ difference at $\delta_{CP} \sim 0.5/\pi$. For combined results of DUNE and T2HK, again GENIE shows around 1σ difference from GiBUU and less than 1σ difference from NuWro at $\delta_{CP} \sim 0.5/\pi$.

The right panel of Fig. 2, shows CP sensitivity when IH is treated as a true hierarchy. For the negative half range ($-1 < \delta_{CP}/\pi < 0$), we notice around 1σ difference between GENIE and NUWro but there is a small difference between GiBUU and NuWro for the T2HK experiment but in the case of DUNE experiment, GENIE and NuWro show little difference but GiBUU shows less than 1σ difference at $\delta_{CP} \sim -0.5/\pi$. When we combine DUNE+T2HK, we see a 1σ difference in GENIE but GiBUU and NuWro show similar results at $\delta_{CP} \sim -0.5/\pi$. Whereas in positive half range ($0 < \delta_{CP}/\pi < 1$), we notice a 1σ difference between GENIE and NUWro but there is a small difference between GiBUU and NuWro for the T2HK but in the case of DUNE, GENIE and NuWro show little difference but GiBUU shows more than 1σ difference at $\delta_{CP} \sim 0.5/\pi$. When we combine DUNE+T2HK, we see 1σ difference between GENIE and NUWro but there is a small difference between GiBUU and NuWro at $\delta_{CP} \sim 0.5/\pi$.

For further understanding of systematics in the generators, we plot the ratio of $\sqrt{\Delta\chi^2}$ in different generators in the Fig. 5 of appendix A.

4.2. Mass hierarchy sensitivity

The quest to understand the real nature of neutrino mass ordering, whether normal or inverted, is one of the most important topics in neutrino physics. The sensitivity of mass hierarchy is evaluated by assuming normal (inverted) hierarchy to be an actual hierarchy and comparing it to inverted (normal) hierarchy using equations (4), (5). As a result, we create hierarchies in true and test values that are diametrically opposed. The mass hierarchy sensitivity is shown in Fig. 3 for both the normal (left panel) and inverted (right panel) instances. The following formula is used to compute the $\Delta\chi^2$ quantity for mass hierarchy sensitivity:

$$\Delta\chi_{MH}^2 = \chi_{IH}^2 - \chi_{NH}^2 \quad (4)$$

$$\Delta\chi_{MH}^2 = \chi_{NH}^2 - \chi_{IH}^2 \quad (5)$$

For the true normal hierarchy case shown in the left panel of Fig. 3. In the negative half range ($-1 < \delta_{CP}/\pi < 0$), we see more than 1σ difference between GENIE and NUWro but there is a small difference between GiBUU and NuWro for the T2HK experiment and in the case of DUNE experiment, GENIE and NuWro show less than 1σ difference but GiBUU shows 2σ difference at $\delta_{CP} \sim -0.5/\pi$. When we combine DUNE+T2HK, we see a 2σ difference in GENIE but GiBUU and NuWro show less difference at $\delta_{CP} \sim -0.5/\pi$. In the case of positive half, ($0 < \delta_{CP}/\pi < 1$) we notice the negligible difference between all generators for the T2HK experiment but for the DUNE experiment, we notice GENIE and NuWro show less than 1σ difference but GiBUU shows around 2σ difference at $\delta_{CP} \sim 0.5/\pi$. For combined results of DUNE and T2HK, we see a 2σ difference between GENIE and NUWro but there is a small difference between GiBUU and NuWro at $\delta_{CP} \sim 0.5/\pi$.

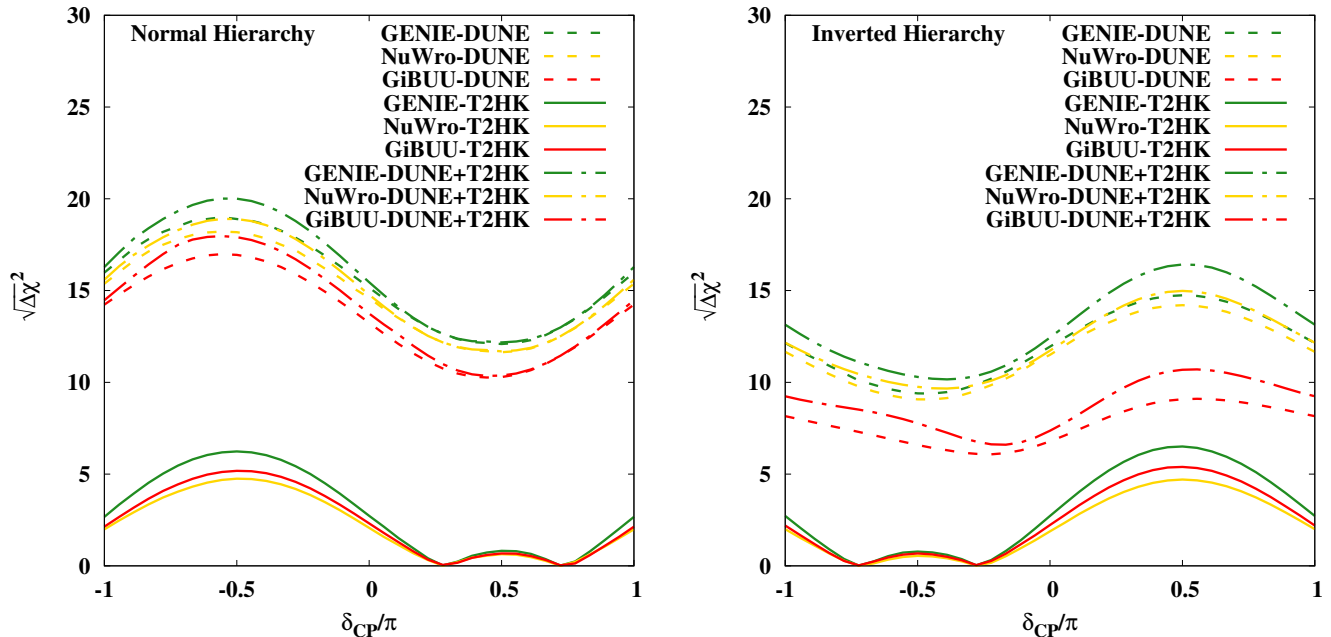


Figure 3: Mass hierarchy sensitivity measurement as a function of the true value of δ_{CP} for NH (left panel) and IH (right panel).

The right panel of Fig. 3, shows CP sensitivity when IH is treated as a true hierarchy. For the negative half range ($-1 < \delta_{CP}/\pi < 0$), we notice the negligible difference in all generators for the T2HK experiment but in the case of the DUNE experiment, GENIE and NuWro show less than 1σ difference but GiBUU shows around 4σ difference at $\delta_{CP} \sim -0.5/\pi$. When we combine DUNE+T2HK, we see around 3σ difference in GENIE but GiBUU and NuWro show 2σ difference at $\delta_{CP} \sim -0.5/\pi$. Whereas in positive half range ($0 < \delta_{CP}/\pi < 1$), we notice around 2σ difference between GENIE and NuWro for the T2HK but in the case of DUNE, GENIE and NuWro show the negligible difference but GiBUU shows more than 5σ difference at $\delta_{CP} \sim 0.5/\pi$. When we combine DUNE+T2HK, we see around 6σ difference between GENIE and GiBUU but there is around 4σ difference between GiBUU and NuWro at $\delta_{CP} \sim 0.5/\pi$.

For further understanding of systematics in the generators, we plot the ratio of $\sqrt{\Delta\chi^2}$ in different generators in the Fig. 6 of appendix A.

4.3. Octant sensitivity

The atmospheric mixing angle θ_{23} is not yet proven to be in the lower octant ($0 < \theta_{23} < \pi/4$)-LO or the higher octant ($\pi/4 < \theta_{23} < \pi/2$)-HO, with a maximum value of $\pi/4$. The development of multiple disconnected zones in the multi-dimensional neutrino oscillation parameter space is the primary challenge in resolving the octant degeneracy. Parameter degeneracy occurs when it is impossible to locate the exact or real answer for a given collection of true values. The test value of θ_{23} is modified in the lower (higher) octant range while doing the octant sensitivity calculations in the lower (higher) octant range. The real value of θ_{23} is 0.703 in the lower octant and 0.867 in the higher octant, although the range of test values for θ_{23} in LO and HO is [0.785, 0.961] and [0.609, 0.785], respectively. The metric $\Delta\chi^2$ for octant sensitivity is defined as

$$\Delta\chi_{octant}^2 = |\chi_{\theta_{23}^{test} > \pi/4}^2 - \chi_{\theta_{23}^{true} < \pi/4}^2| \quad (6)$$

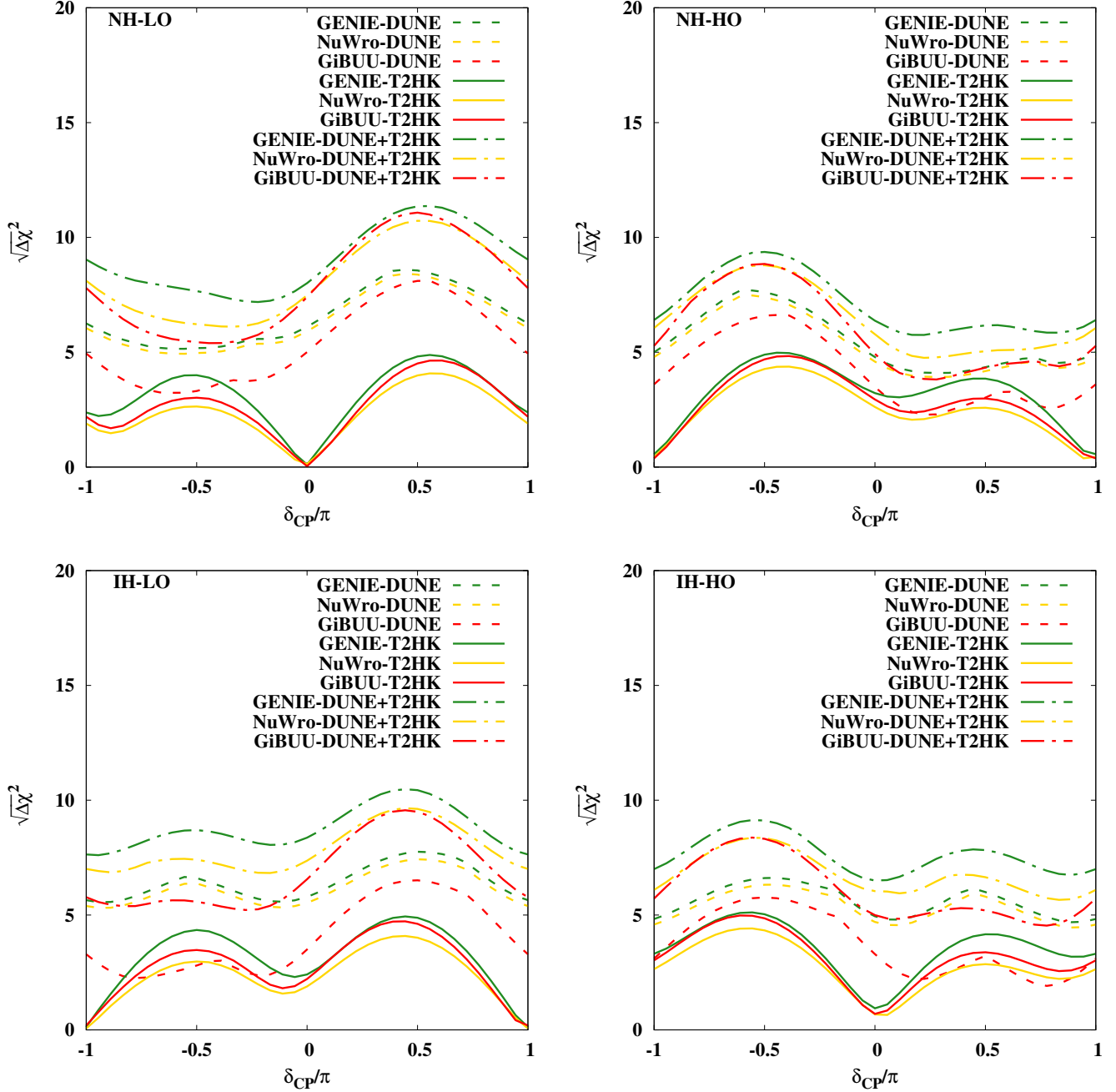


Figure 4: Octant sensitivity measurement as a function of the true value of δ_{CP} for NH-LO (top left), NH-HO (top right), IH-LO (bottom left) and IH-HO (bottom right).

In Fig. 4, the top and bottom panels, we show the results for four true hierarchy and octant configurations, namely NH-LO, NH-HO, IH-LO, and IH-HO. For the NH-LO scenario (top left panel of Fig. 4), in the negative half range ($-1 < \delta_{CP}/\pi < 0$), we see more than 1σ difference between GENIE and NuWro but there is a small difference

between GiBUU and NuWro for the T2HK experiment and in the case of DUNE experiment, GENIE and NuWro show the negligible difference but GiBUU shows 2σ difference at $\delta_{CP} \sim -0.5/\pi$. When we combine DUNE+T2HK, we see a 2σ difference in GENIE but GiBUU and NuWro show less difference at $\delta_{CP} \sim -0.5/\pi$. In the case of positive half ($0 < \delta_{CP}/\pi < 1$), we notice less than 1σ difference between GENIE and NuWro for the T2HK experiment but for the DUNE experiment, we notice a small difference in all generators at $\delta_{CP} \sim 0.5/\pi$. For combine results of DUNE and T2HK, we see the negligible difference at $\delta_{CP} \sim 0.5/\pi$. For a better understanding of systematics in the generators, we plot the ratio of $\sqrt{\Delta\chi^2}$ in different generators in Fig. 7 (top left panel) of appendix A.

For the NH-HO case (top right panel of Fig. 4), in the negative half range ($-1 < \delta_{CP}/\pi < 0$), we see a small difference in all generators for the T2HK but in the case of the DUNE, GENIE and NuWro show similar results but GiBUU shows more than 1σ variations at $\delta_{CP} \sim -0.5/\pi$. When we combine DUNE+T2HK, we see a small difference in all generators at $\delta_{CP} \sim -0.5/\pi$. In the case of positive half ($0 < \delta_{CP}/\pi < 1$), we notice less than 1σ difference between GENIE and GiBUU for the T2HK and more than 1σ difference for DUNE experiment at $\delta_{CP} \sim 0.5/\pi$ between GENIE and GiBUU but GENIE and NuWro show almost similar results. For combined results of DUNE and T2HK, we notice around 2σ difference between GENIE and GiBUU at $\delta_{CP} \sim 0.5/\pi$. For a better understanding of systematics in the generators, we plot the ratio of $\sqrt{\Delta\chi^2}$ in different generators in Fig. 7 (top right panel) of appendix A.

For the IH-LO case (bottom left panel of Fig. 4), in the negative half range ($-1 < \delta_{CP}/\pi < 0$), we see around 1σ difference between GENIE and NuWro and the negligible difference between GiBUU and NuWro for the T2HK but in the case of DUNE, GENIE and NuWro show similar results but GiBUU shows around 4σ variations at $\delta_{CP} \sim -0.5/\pi$. When we combine DUNE+T2HK, we see NuWro shows 1σ difference and GiBUU shows 3σ variations from GENIE at $\delta_{CP} \sim -0.5/\pi$. In the case of positive half ($0 < \delta_{CP}/\pi < 1$), we notice around 1σ difference between GENIE and NuWro and negligible between GiBUU and GENIE for the T2HK and more than 1σ difference between GENIE and GiBUU for the DUNE experiment at $\delta_{CP} \sim 0.5/\pi$. For combined results of DUNE and T2HK, we notice GiBUU shows 1σ and NuWro shows less than 1σ difference from GENIE at $\delta_{CP} \sim 0.5/\pi$. For a better understanding of systematics in the generators, we plot the ratio of $\sqrt{\Delta\chi^2}$ in different generators in Fig. 7 (bottom left panel) of appendix A.

For the IH-HO case (bottom right panel of Fig. 4), in the negative half range ($-1 < \delta_{CP}/\pi < 0$), we notice less than 1σ difference between GENIE and NuWro and the negligible between GiBUU and GENIE for the T2HK and less than 1σ difference between GENIE and GiBUU for the DUNE experiment at $\delta_{CP} \sim 0.5/\pi$. For combined results of DUNE and T2HK, we notice GiBUU shows less than 1σ and NuWro shows less than 1σ difference from GENIE at $\delta_{CP} \sim 0.5/\pi$. In the case of positive half ($0 < \delta_{CP}/\pi < 1$), we see around 1σ difference between GENIE and NuWro and a negligible difference between GiBUU and NuWro for the T2HK but in the case of DUNE, GENIE and NuWro show similar results but GiBUU shows around 3σ variations at $\delta_{CP} \sim -0.5/\pi$. When we combine DUNE+T2HK, we see NuWro shows 1σ difference and GiBUU shows more than 2σ variations from GENIE at $\delta_{CP} \sim -0.5/\pi$. For a better understanding of systematics in the generators, we plot the ratio of $\sqrt{\Delta\chi^2}$ in different generators in Fig. 7 (bottom right panel) of appendix A.

5. Summary and conclusions

In this paper, we have studied the impact of cross-sectional uncertainty on determining the CP-violation, mass hierarchy, and octant degeneracy in the T2HK, DUNE, and DUNE+T2HK using GENIE, NuWro, and GiBUU nuclear models. Because nuclear effects are not completely known, different generators utilize different estimates to account for them, resulting in a variety of results. Because there is insufficient cross-section data to comprehend the existing nuclear effects, it is necessary to determine cross-section for diverse nuclei and update the current cross-section data. Every target nucleus' nuclear structure (mass number, atomic number) is unique, posing a significant problem in the correct computation of neutrino-nucleon cross-section. From our analysis, we notice that GENIE gives the better result as a comparison to NuWro and GiBUU for both DUNE and T2HK experiments. NuWro shows better results for DUNE experiment than GiBUU but for T2HK experiment GiBUU shows better results than NuWro. When we combine the results of DUNE and T2HK, GENIE gives better results as a comparison to NuWro and GiBUU. From these results, we can conclude that for higher energy experiments it is better to choose a GENIE generator. The physics results' emphasis on the generators' selection will limit the physics analysis targets.

A. Appendix

1. CP violation sensitivity

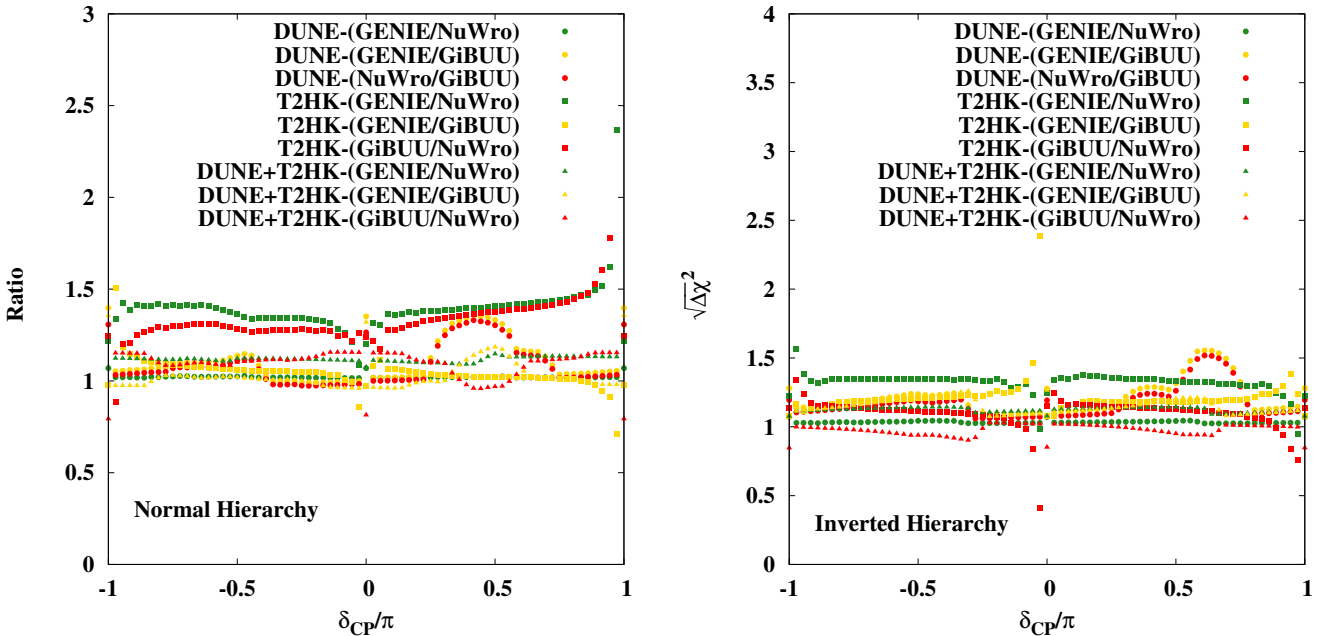


Figure 5: Ratio of generators for NH (left panel) and IH (right panel) for T2HK (square), DUNE (circle), and T2HK+DUNE (triangle) experiments.

2. Mass hierarchy sensitivity

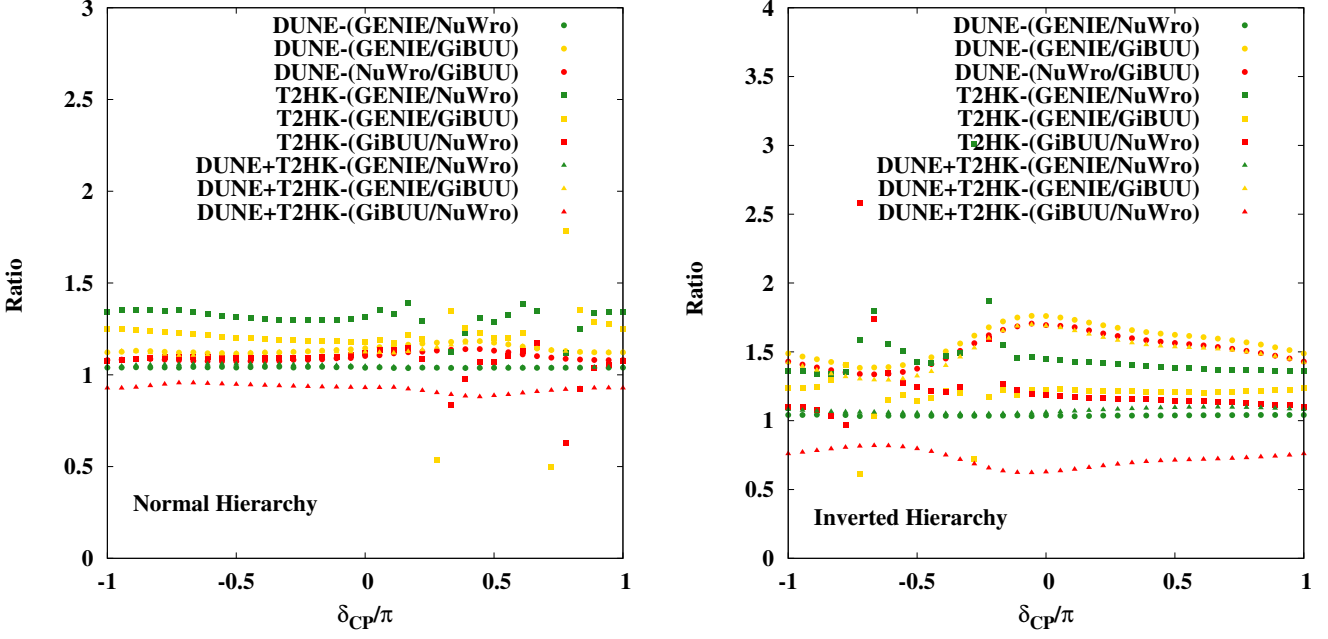


Figure 6: Mass hierarchy sensitivity measurement as a function of the true value of δ_{CP} for NH (left panel) and IH (right panel).

3. Octant sensitivity

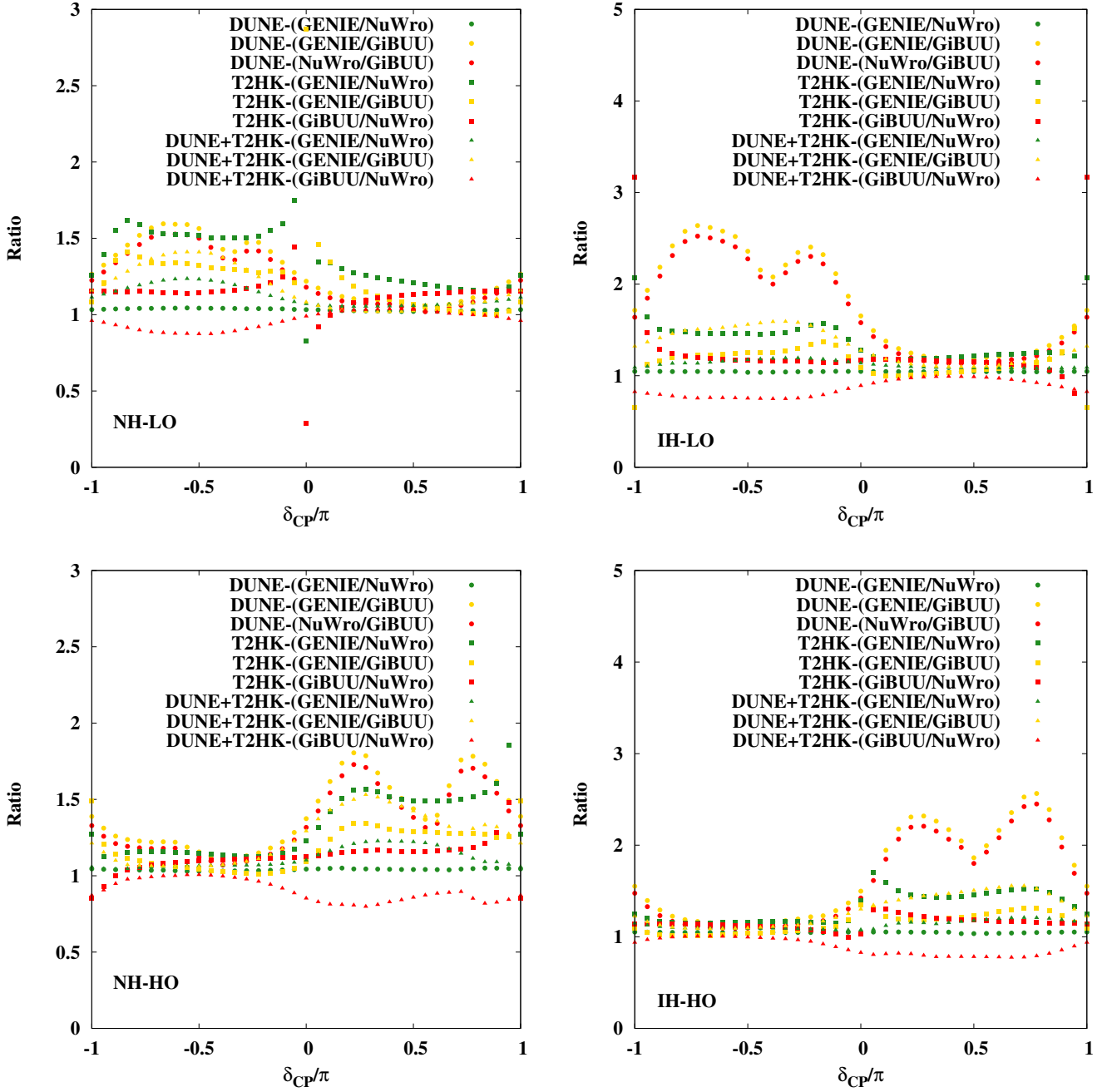


Figure 7: Octant sensitivity measurement as a function of the true value of δ_{CP} for NH-LO (top left), NH-HO (top right), IH-LO (bottom left) and IH-HO (bottom right).

References

-
- [1] F.P. An, et al., Observation of electron-antineutrino disappearance at Daya Bay, Phys. Rev. Lett. 108 (2012) 171803.
<https://doi.org/10.1103/PhysRevLett.108.171803>.

- [2] F.P. An, et al., Improved Measurement of Electron Antineutrino Disappearance at Daya Bay, *Chin. Phys. C* 37 (2013) 011001. <https://doi.org/10.1088/1674-1137/37/1/011001>.
- [3] J.K. Ahn et al., Observation of Reactor Electron Antineutrino Disappearance in the RENO Experiment, *Phys. Rev. Lett.* 108 (2012) 191802. <https://doi.org/10.1103/PhysRevLett.108.191802>.
- [4] G. Engelhard, Y. Grossman, Y. Nir, Relating leptogenesis parameters to light neutrino masses, *JHEP* 07 (2007) 029. <https://doi.org/10.1088/1126-6708/2007/07/029>.
- [5] S. Pascoli, S.T. Petcov, and A. Riotto, Connecting Low Energy Leptonic CP-violation to Leptogenesis, *Phys. Rev. D* 75 (2007) 083511. <https://doi.org/10.1103/PhysRevD.75.083511>.
- [6] R. Devi, J. Singh, and B. Potukuchi. Uncertainties due to hadronic production in FSI at LBNF, arXiv:2110.00117 [hep-ph] (2021).
- [7] P. Huber, M. Mezzetto, and T. Schwetz, On the impact of systematical uncertainties for the CP violation measurement in superbeam experiments, *JHEP* 03 (2008) 021. <https://doi.org/10.1088/1126-6708/2008/03/021>.
- [8] P. Coloma, P. Huber, J. Kopp, and W. Winter, Systematic uncertainties in long-baseline neutrino oscillations for large θ_{13} . *Phys. Rev. D* 87 (2013) 033004. <https://doi.org/10.1103/PhysRevD.87.033004>.
- [9] D. Harris et al. (MINERvA Collaboration), Neutrino Scattering Uncertainties and their Role in Long Baseline Oscillation Experiments, arXiv:hep-ex/0410005 (2004).
- [10] M. Martini, M. Ericson, and G. Chanfray, Neutrino energy reconstruction problems and neutrino oscillations, *Phys. Rev. D* 85 (2012) 093012. <https://doi.org/10.1103/PhysRevD.85.093012>.
- [11] M. Martini, M. Ericson, and G. Chanfray, Energy reconstruction effects in neutrino oscillation experiments and implications for the analysis, *Phys. Rev. D* 87 (2013) 013009. <https://doi.org/10.1103/PhysRevD.87.013009>.
- [12] O. Lalakulich, U. Mosel, and K. Gallmeister, Neutrino energy reconstruction in quasielastic-like scattering in the Mini-BooNE and T2K experiments, *Phys. Rev. C* 86 (2012) 054606. <https://doi.org/10.1103/PhysRevC.86.054606>.
- [13] U. Mosel, O. Lalakulich, and K. Gallmeister, Energy Reconstruction in the Long-Baseline Neutrino Experiment, *Phys. Rev. Lett.* 112 (2014) 151802. <https://doi.org/10.1103/PhysRevLett.112.151802>.
- [14] S. Naaz, A. Yadav, J. Singh and R.B. Singh, Effect of final state interactions on neutrino energy reconstruction at DUNE, *Nucl. Phys. B* 933 (2018) 40. <https://doi.org/10.1016/j.nuclphysb.2018.05.018>.
- [15] O. Lalakulich, K. Gallmeister and U. Mosel, Neutrino and antineutrino induced reactions with nuclei between 1 and 50 GeV, *Phys. Rev. C* 86 (2012) 014607. <https://doi.org/10.1103/PhysRevC.86.014607>.
- [16] C. Andreopoulos et al., The GENIE Neutrino Monte Carlo Generator, *Nucl. Instrum. Meth. A* 614 (2010) 87. <https://doi.org/10.1016/j.nima.2009.12.009>.
- [17] T. Golan, C. Juszczak, and J.T. Sobczyk, Effects of final-state interactions in neutrino-nucleus interactions, *Phys. Rev. C* 86 (2012) 015505. <https://doi.org/10.1103/PhysRevC.86.015505>.
- [18] O. Buss et al., Transport-theoretical Description of Nuclear Reactions, *Phys. Rept.* 512 (2012) 1. <https://doi.org/10.1016/j.physrep.2011.12.001>.
- [19] R. Brun, and F. Rademakers, ROOT - An Object Oriented Data Analysis Framework, *Nucl. Inst. Meth. A* 389 (1997) 81. [https://doi.org/10.1016/S0168-9002\(97\)00048-X](https://doi.org/10.1016/S0168-9002(97)00048-X).
- [20] D. Drakoulakos et al. (Minerva Collaboration), Proposal to perform a high-statistics neutrino scattering experiment using a fine-grained detector in the NuMI beam, arxiv:hep-ex/0405002 (2004).
- [21] P. Adamson et al. (MINOS Collaboration), Study of muon neutrino disappearance using the Fermilab Main Injector neutrino beam, *Phys. Rev. D* 77 (2008) 072002. <https://doi.org/10.1103/PhysRevD.77.072002>.
- [22] H. Chen et al. (MicroBooNE Collaboration), Proposal for a New Experiment Using the Booster and NuMI Neutrino Beamlines: MicroBooNE, FERMILAB-PROPOSAL-0974 (2007).
- [23] D. Ayres et al. (NOvA Collaboration), NOvA: Proposal to Build a 30 Kiloton Off-Axis Detector to Study $\nu_\mu \rightarrow \nu_e$

Oscillations in the NuMI Beamline, arxiv:hep-ex/0503053 (2004).

- [24] A. Bodek and J.L. Ritchie, Further studies of fermi motion effects in lepton scattering from nuclear targets, *Phys. Rev. D* 24 (1981) 1400. <https://doi.org/10.1103/PhysRevD.24.1400>.
- [25] C.H. Llewellyn Smith, Neutrino reactions at accelerator energies, *Phys. Rept.* 3 (1972) 261. [https://doi.org/10.1016/0370-1573\(72\)90010-5](https://doi.org/10.1016/0370-1573(72)90010-5).
- [26] R. Bradford, A. Bodek, H.S. Budd, and J. Arrington, A new parameterization of the nucleon elastic form factors, *Nucl. Phys. Proc. Suppl.* 159 (2006) 127. <https://doi.org/10.1016/j.nuclphysbps.2006.08.028>.
- [27] D. Rein and L.M. Sehgal, Neutrino excitation of baryon resonances and single pion production, *Ann. Phys.* 133 (1981) 79. [https://doi.org/10.1016/0003-4916\(81\)90242-6](https://doi.org/10.1016/0003-4916(81)90242-6).
- [28] R. P. Feynman, M. Kislinger, and F. Ravndal, Current matrix elements from a relativistic quark model, *Phys. Rev. D* 3 (1971) 2706. <https://doi.org/10.1103/PhysRevD.3.2706>.
- [29] A. Bodek and U.K. Yang, Higher twist, $\xi(\omega)$ scaling, and effective LO PDFs for lepton scattering in the few GeV region, *J. Phys. G* 29 (2003) 1899. <https://doi.org/10.1088/0954-3899/29/8/369>.
- [30] H. Budd, A. Bodek, and J. Arrington, Modeling Quasi-elastic Form Factors for Electron and Neutrino Scattering, arxiv:hep-ex/0308005 (2003).
- [31] W.M. Alberico, S.M. Bilenky, C. Giunti, and K.M. Graczyk, Electromagnetic form factors of the nucleon: New fit and analysis of uncertainties, *Phys. Rev. C* 79 (2009) 065204. <https://doi.org/10.1103/PhysRevC.79.065204>.
- [32] K.M. Graczyk, D. Kielczewska, P. Przewlocki, and J.T. Sobczyk, C_5^A axial form factor from bubble chamber experiments, *Phys. Rev. D* 80 (2009) 093001. <https://doi.org/10.1103/PhysRevD.80.093001>.
- [33] C. Juszczak, J.A. Nowak, and J.T. Sobczyk, Simulations from a new neutrino event generator, *Nucl. Phys. Proc. Suppl.* 159 (2006) 211. <https://doi.org/10.1016/j.nuclphysbps.2006.08.069>.
- [34] A. Bodek, U.K. Yang, Modeling deep inelastic cross sections in the few GeV region, *Nucl. Phys. B Proc.(Suppl)* 112 (2002) 70. [https://doi.org/10.1016/S0920-5632\(02\)01755-3](https://doi.org/10.1016/S0920-5632(02)01755-3).
- [35] K. Gallmeister et al., Neutrino-induced reactions on nuclei, *Phys. Rev. C* 94 (2016) 035502. <https://doi.org/10.1103/PhysRevC.94.035502>.
- [36] A. Bodek, S. Avvakumov, R. Bradford, and H.S. Budd, Modeling Atmospheric Neutrino Interactions: Duality Constrained Parameterization of Vector and Axial Nucleon Form Factors, 30th International Cosmic Ray Conference (ICRC 2007), arXiv:0708.1827 [hep-ex].
- [37] D. Drechsel, L. Tiator, Threshold pion photoproduction on nucleons, *J. Phys. G* 18 (1992) 449. <https://doi.org/10.1088/0954-3899/18/3/004>.
- [38] D. Rein, L. Sehgal, Coherent production of photons by neutrinos, *Phys. Lett. B* 104 (1981) 394. [https://doi.org/10.1016/0370-2693\(81\)90706-1](https://doi.org/10.1016/0370-2693(81)90706-1).
- [39] O. Lalakulich, K. Gallmeister, U. Mosel, Neutrino nucleus reactions within the GiBUU model, *J. Phys. Conf. Ser.* 408 (2013) 012053. <https://doi.org/10.1088/1742-6596/408/1/012053>.
- [40] P. Huber, M.Lindner and W. Winter, From parameter space constraints to the precision determination of the leptonic Dirac CP phase, *JHEP* 05 (2005) 020. <https://doi.org/10.1088/1126-6708/2005/05/020>.
- [41] P. Huber, M.Lindner, T. Schwetz and W. Winter, First hint for CP violation in neutrino oscillations from upcoming superbeam and reactor experiments, *JHEP* 11 (2009) 044. <https://doi.org/10.1088/1126-6708/2009/11/044>.
- [42] P. Huber, J. Kopp, M. Lindner, M. Rolinec, W. Winter. <https://www.mpi-hd.mpg.de/personalhomes/globes/>.
- [43] K. Abe et al. (Hyper-Kamiokande Proto-Collaboration), Hyper-Kamiokande Design Report, KEK Preprint 2016-21, ICRR-Report-701-2016-1, 2016.
- [44] P. Huber, M. Lindner, and W. Winter, Superbeams versus neutrino factories, *Nucl. Phys. B* 645 (2002) 3. [https://doi.org/10.1016/S0550-3213\(02\)00825-8](https://doi.org/10.1016/S0550-3213(02)00825-8).

- [45] M. Ishitsuka, et al., Resolving the neutrino mass hierarchy and CP degeneracy by two identical detectors with different baselines, *Phys. Rev. D* 72 (2005) 033003. <https://doi.org/10.1103/PhysRevD.72.033003>.
- [46] J. Singh et al. Quantifying multinucleon effect in Argon using high-pressure TPC. *Nucl. Phys. B* 957, 115103 (2020).
- [47] B. Abi et al. Long-baseline neutrino oscillation physics potential of the DUNE experiment. *Eur. Phys. J.* 80, 978 (2020). [DOI:<https://doi.org/10.1140/epjc/s10052-020-08456-z>].
- [48] <http://home.fnal.gov/ljf26/DUNE2015CDRFluxes/>.
- [49] C. Adams, (LBNE Collaboration) The Long-Baseline Neutrino Experiment: Exploring Fundamental Symmetries of the Universe, FERMILAB-PUB-14-022, arxiv:1307.7335 (2013).
- [50] I. Esteban, et al., Global analysis of three-flavour neutrino oscillations: synergies and tensions in the determination of θ_{23} , δ_{CP} , and the mass ordering, *JHEP* 01 (2019) 106. [https://doi.org/10.1007/JHEP01\(2019\)106](https://doi.org/10.1007/JHEP01(2019)106).
- [51] Y. Itow et al. (T2K Collaboration), The JHF-Kamioka neutrino project (arXiv:hep-ex/0106019) (2007).
- [52] K. Abe, et al., A Long Baseline Neutrino Oscillation Experiment Using J-PARC Neutrino Beam and Hyper-Kamiokande, arXiv:1412.4673 [physics.ins-det] (2014).
- [53] K.N. Deepthi, C. Soumya, R. Mohanta, Revisiting the sensitivity studies for leptonic CP violation and mass hierarchy with T2K, NO ν A and LBNE experiments, *New J. Phys.* 17 (2015) 023035. <https://doi.org/10.1088/1367-2630/17/2/023035>.
- [54] K. Chakraborty, K.N. Deepthi, S. Goswami, Spotlighting the sensitivities of T2HK, T2HKK and DUNE, *Nucl. Phys. B* 937 (2018) 303. <https://doi.org/10.1016/j.nuclphysb.2018.10.013>.
- [55] S. Nagu, et al., Impact of cross-sectional uncertainties on DUNE sensitivity due to nuclear effects, *Nucl. Phys. B* 951 (2020) 114888. <https://doi.org/10.1016/j.nuclphysb.2019.114888>.